

Nuclear structure of ^{181}Au studied via β^+/EC decay of ^{181}Hg at ISOLDE

M. Sedlák^{1,a}, M. Venhart¹, J. L. Wood², V. Matoušek¹, M. Balogh¹,
A. J. Boston³, T. E. Cocolios⁴, L. J. Harkness-Brennan³, R.-D. Herzberg³,
D. T. Joss³, D. S. Judson³, J. Kliman¹, R. D. Page³, A. Patel³, K. Petrík¹,
M. Veselský¹

¹ Institute of Physics, Slovak Academy of Sciences, SK-84511 Bratislava, Slovakia

² Department of Physics, Georgia Institute of Technology, Atlanta, Georgia 30332, USA

³ Oliver Lodge Laboratory, University of Liverpool, Liverpool, L69 7ZE, United Kingdom

⁴ KU Leuven, Instituut voor Kern- en Stralingsfysica, B-3001 Leuven, Belgium

Received: date / Accepted: date

Abstract

1 Introduction

The nuclear structure of the odd-mass Au isotopes is distinguished by three major features: it is the longest chain of odd-mass isotopes for which excited state information is now available; there are proton-hole states that exhibit near constant energies over a change in neutron number corresponding to some 30 mass units; and there are multiple coexisting intruder states (involving proton-particle excitations across the $Z = 82$ closed shell). This picture has emerged from studies of high-spin states using in-beam γ -ray spectroscopy [1–18] and studies of low-spin and medium-spin states by β decay of Hg isotopes [19–29], atomic-beam magnetic resonance technique [30–32], in-source laser spectroscopy [33], α decay of Tl isotopes [34], and isomeric state decays in the Au isotopes [35,36]. Details of many of the intruder states have been given in reviews [37–39].

For the extremely neutron-deficient odd-mass Au isotopes, the excited-state data are progressively more limited with decreasing mass number. Nevertheless, a dramatic feature has been characterized: in ^{177}Au there is a band consistent with very strong deformation, which is unique in the odd-mass Au isotopes to this nucleus [13]. However, below ^{183}Au there are almost no data for low-spin states. Herein, we report results on low-spin states in ^{181}Au via radioactive decay of ^{181}Hg ($T_{1/2} = 3.6\text{ s}$, $J^\pi = 1/2^-$, $Q(\beta^+) = -7862(18)\text{ keV}$). This has necessitated a major advance in technique for odd-mass decay scheme spectroscopy, which has recently been developed [40]. The primary need for this advance is the

large α -decay branch of ^{181}Hg : this results in decays in multiple isobaric chains as depicted in Fig. 1, with the consequence that previous work [27] has made incorrect assignments of γ rays to the β -decaying and α -decaying species. Thus, prior to the present study, a decay scheme for $^{181}\text{Hg} \rightarrow ^{181}\text{Au}$ has not been available and, indeed, the strongest γ rays in the decay scheme were not identified due to unresolved multiplets involving transitions in other isotopes.

2 Experimental details

The experiment was performed at the ISOLDE facility, which is active at CERN. It is a premier facility delivering radioactive-ion beams of various elements and isotopes. A bunched proton beam with energy of 1.4 GeV and typical intensity of $1.5\text{ }\mu\text{A}$ impinged on a molten lead target, inducing processes such as spallation, fission, and fragmentation. These processes produced a variety of isotopes in the target. Due to the high temperature of the target, reaction products were diffused out of the target and subsequently ionised with a plasma ion source, and extracted with a 30 kV potential. The General Purpose Separator, which has one bending magnet, was used for mass separation. Production, and extraction of ^{181}Pb , ^{181}Tl , and ^{181}Au was very low and Hf-Pt elements were not extracted at all, due to their refractory nature. Therefore, a practically pure ^{181}Hg beam was delivered.

Samples of ^{181}Hg were created by the deposition of the radioactive-ion beam onto the metallic tape of the TATRA spectrometer [41] installed at the LA1 beam line of the ISOLDE facility. Subsequently, the sample was transported by rapid motion of the tape into the

^aCorresponding author, e-mail: matus.sedlak@savba.sk

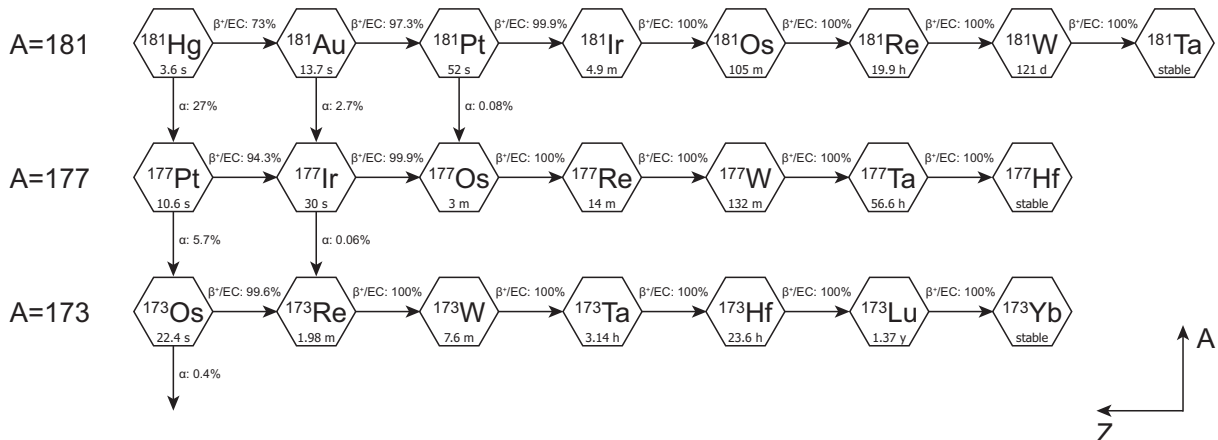


Fig. 1 Decay branches of ^{181}Hg and its daughter isotopes. The data are taken from *Evaluated Nuclear Structure Data File*.

measurement chamber. Two standard coaxial germanium detectors with relative efficiency of 70 % and a single Broad Energy Germanium detector [42], type BE2020, were positioned around the sample located at the measurement point. Source-to-detector distances were of 5 cm. All detectors were calibrated for energy and intensity of γ -ray lines with standard sources and procedures.

The data were acquired with the fully-digital acquisition system, based on the commercial Pixie-16 14 bit, 250 MHz digitisers. The data were collected from preamplifiers of each detector separately, pulse height was reconstructed on an even-by-event basis, timestamped and stored as 32 768 channel spectrum. The coincidence relationships were investigated offline, using the timestamp information. Signals from the BE2020 BEGe detector were amplified prior to digitisation (without shaping). The dynamical range of the digitiser covered the range up to approximately 920 keV, which gives 29 eV per channel in the singles spectrum. This allowed for enhanced separation of γ rays that are close in energy via the shapes of peaks.

3 Experimental results

Fig. 2 gives part of the spectrum detected with the BE2020 BEGe detector within a time window of 12 s after transportation of the sample into the measurement position. Characteristic X-rays of all elements between tantalum and gold are clearly visible. Long-lived species were present either due to accumulation of the activity on the tape from a preceding study of ^{183}Hg decay, performed within the same experiment, or by contamination of the measurement chamber. If α decay occurs and the α particle is emitted into the tape, the recoiling nucleus can be ejected from the tape. Therefore,

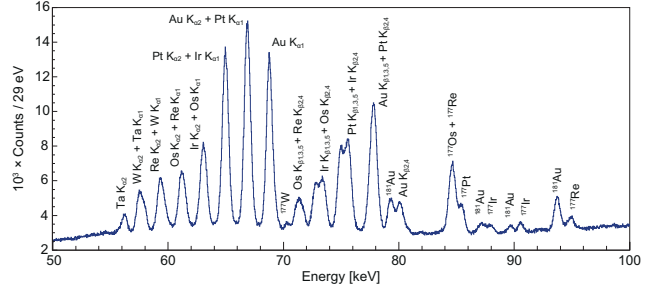


Fig. 2 Part of the γ -ray singles spectrum detected with the BE2020 BEGe detector, within a time window of 12 s after transportation of the sample into the measurement position. Characteristic $K_{\alpha 1}$, and $K_{\alpha 2}$ X rays of Au, Pt, Ir, Os, Re, W, and Ta are marked. Other peaks are due to characteristic K_{β} radiation and low-energy γ rays.

for identification of γ rays related to the mother decay of ^{181}Hg , a method based on the time structure of the data was used. The method is described in [13] and was successfully used in the ^{183}Hg decay study [40]. Compared to that study, more contaminating isotopes with various half lives are present here. Therefore, the resulting spectra have to be analysed very carefully, since some peaks may not be suppressed, or suppressed only partially, or can create “negative” peaks.

Fig. 3a gives the part of the γ -ray singles spectrum detected with the BE2020 BEGe detector within a time window of 12 s after transportation of the sample into the measurement position. The deconvoluted spectrum is given in Fig. 3b. It clearly demonstrates the separation power of the technique used in the present work.

Fig. 4 gives a sample singles spectrum from the coaxial germanium detector, depicting the data quality at high energy. Also for the coaxial detector, the same deconvolution method can be used. Part of the singles spectrum, together with deconvoluted spectrum is given in Fig. 5.

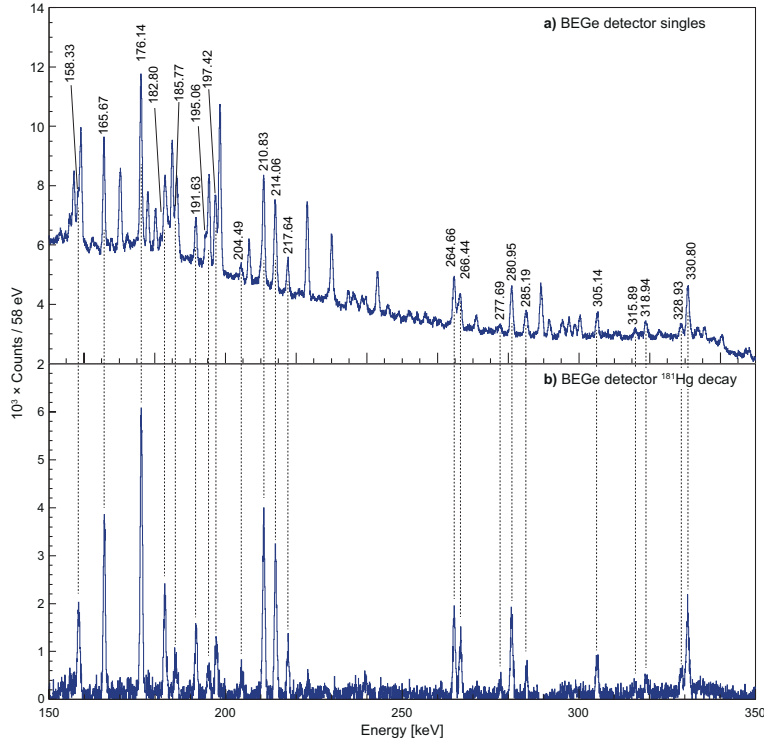


Fig. 3 **a)** Part of the γ -ray singles spectrum detected with the BE2020 BEGe detector, within a time window of 12 s after transportation of the sample into the measurement position. Transitions attributed to the decay of ^{181}Hg are denoted with their energies. **b)** Part of the spectrum of the γ -ray singles attributed to the ^{181}Hg decay, deconvoluted from the total spectrum using the timestructure of the data, see the text for details.

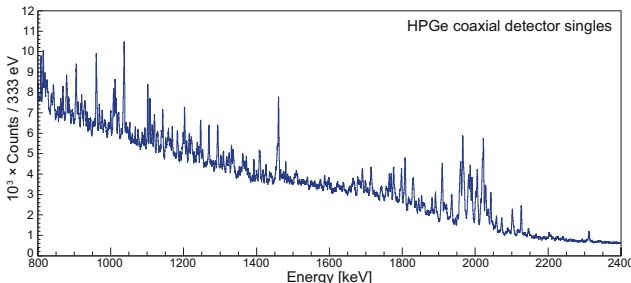


Fig. 4 Part of the γ -ray singles spectrum detected with the coaxial germanium detector, within a time window of 12 s after transportation of the sample into the measurement position

A list of γ rays associated with the ^{181}Hg , observed in the present work, is given in Table 1. Previous study of the ^{181}Hg decay [27] reported 20 γ rays. Out of these 20 transitions, only 7 were observed also in the present experiment: 147.48, 214.06, 239.69 (all from α decay), 165.67, 210.83, 217.64, 280.95, and 330.80 keV. Other transitions reported in [27] are not confirmed by the present study. The study [27] reported also 30.8 and 42.5 keV transitions. In the present experiment, γ rays with such low energies could not be detected due to a 50 keV threshold. A dedicated experiment is needed to clarify origin and character of these transitions. Most

notably, the study [27] does not report 111.34 and 113.11 keV transitions. The 113.11 keV is the strongest γ ray associated with the β^+/EC decay of the ^{181}Hg , see Table 1. Authors of the study [27] state explicitly that “lines belonging to the $^{181}\text{Pt} \rightarrow ^{181}\text{Ir}$ decay were present with high intensity in all the spectra”. The strongest γ ray associated with this decay has an energy of 112.2 keV [27], i.e., between the 111.34 and 113.11 keV transitions of the ^{181}Hg decay. In the previous study, n-type Hyperpure Germanium detectors were used. They have inferior energy resolution compared to BEGe at these energies and moreover, they were operated at low gain (according to published spectra approximately 0.4 keV per ADC channel). Note that our procedure uses a gain on 29 eV per channel: this ensures necessary energy precision and provides critical energy information to assign the many low-energy lines to the various decay daughter species.

The proposed level scheme constructed on the basis of the Rydberg-Ritz analysis and coincidence relationships is given in Fig. 6 and is discussed further in the text.

Fig. 7a gives a spectrum of γ -ray singles detected with the BE2020 BEGe detector, within a time window of 12 s after transportation of the sample into measurement position. Peaks were fitted with Gaussian shapes

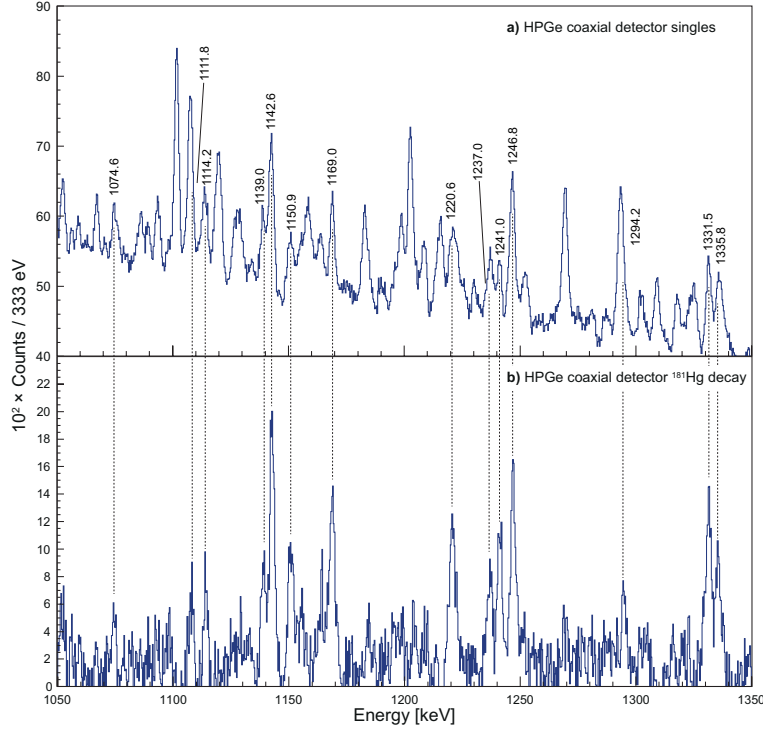


Fig. 5 a) Part of the γ -ray singles spectrum detected with the coaxial germanium detector, within a time window of 12 s after transportation of the sample into the measurement position. Transitions attributed to the decay of ^{181}Hg are denoted with their energies. b) Part of the spectrum of the γ -ray singles attributed to the ^{181}Hg decay, deconvoluted from the total spectrum using the timestructure of the data, see the text for details.

to obtain γ -ray energies and intensities. A reduced χ^2 is 1.03 for the energy fit, suggests that fitted line shapes and background very well reproduce the data. Fig. 7b gives deconvoluted spectra using the time structure of the data, see discussion above and [13]. The green spectrum gives γ rays associated with the ^{181}Hg decay, while the orange spectrum gives γ rays associated with daughter activities. Prominent in the green spectrum are the 111.34 and 113.11 keV transitions. The 115.65 keV transition also remains in the green spectrum, however this is a known transition of the ^{177}W isotope [44]. Parameters of the deconvolution were tuned to subtract the ^{181}Au transitions (dominant contamination) and therefore the 115.65 keV peak remains in the spectrum. The 112.2 keV γ ray is a known transition of the ^{181}Pt decay [28]. It is slightly over-subtracted because of the procedure parameter settings. The 113.11 keV transition is the strongest associated with the ^{181}Hg β^+ /EC decay, see Table 1. Therefore it has to be located in the bottom part of the level scheme, most probably feeding the ground state.

Coincidence relationships of the 111.34 and 113.11 keV transitions were investigated. These transitions were found not to coincide with each other. Fig. 8 gives the projection of the γ - γ matrix with gates on the 1909.5, 767.11, and 590.90 keV transitions. The Figure shows

spectra gated with the coaxial germanium detector, as observed with the BE2020 BEGe detector. The 113.11 and 111.34 keV γ -ray pair are observed in all three spectra, although the statistics are low, especially in the 767.11 keV gate. Therefore, the 113.11 and 111.34 keV transitions are interpreted as deexcitations of the 113.11 keV state in ^{181}Au , feeding the ground state and first excited state. The excitation energy of 1.77 keV for the first excited state is established as an energy difference of the 113.11, and 111.34 keV transitions, while it is supported by the energy difference of the 266.44 and 264.66 keV transitions within statistical uncertainties.

The $1h_{11/2}$ is an unique-parity orbital and therefore it is almost unaffected by configuration mixing. Unique-parity configurations form isolated groups of states that are connected with strong transitions and only rarely deexcite into different configurations. Typically, the band head is an isomeric state [24]. Such states were identified in all known odd-Au isotopes, with the exception of $^{179,181}\text{Au}$ [19, 23, 24, 26]. Fig. 9 gives the projection of the γ - γ matrix with gates on a) 305.14, b) 607.76, and c) 760.18 keV transitions. All three coincidence gates show a 158.33 keV transition, which is interpreted as decay of the $11/2^-$ band head of the $1h_{11/2}$ configuration, which is isomeric as in the heavy isotopes. The 305.14 keV γ ray is interpreted as a de-

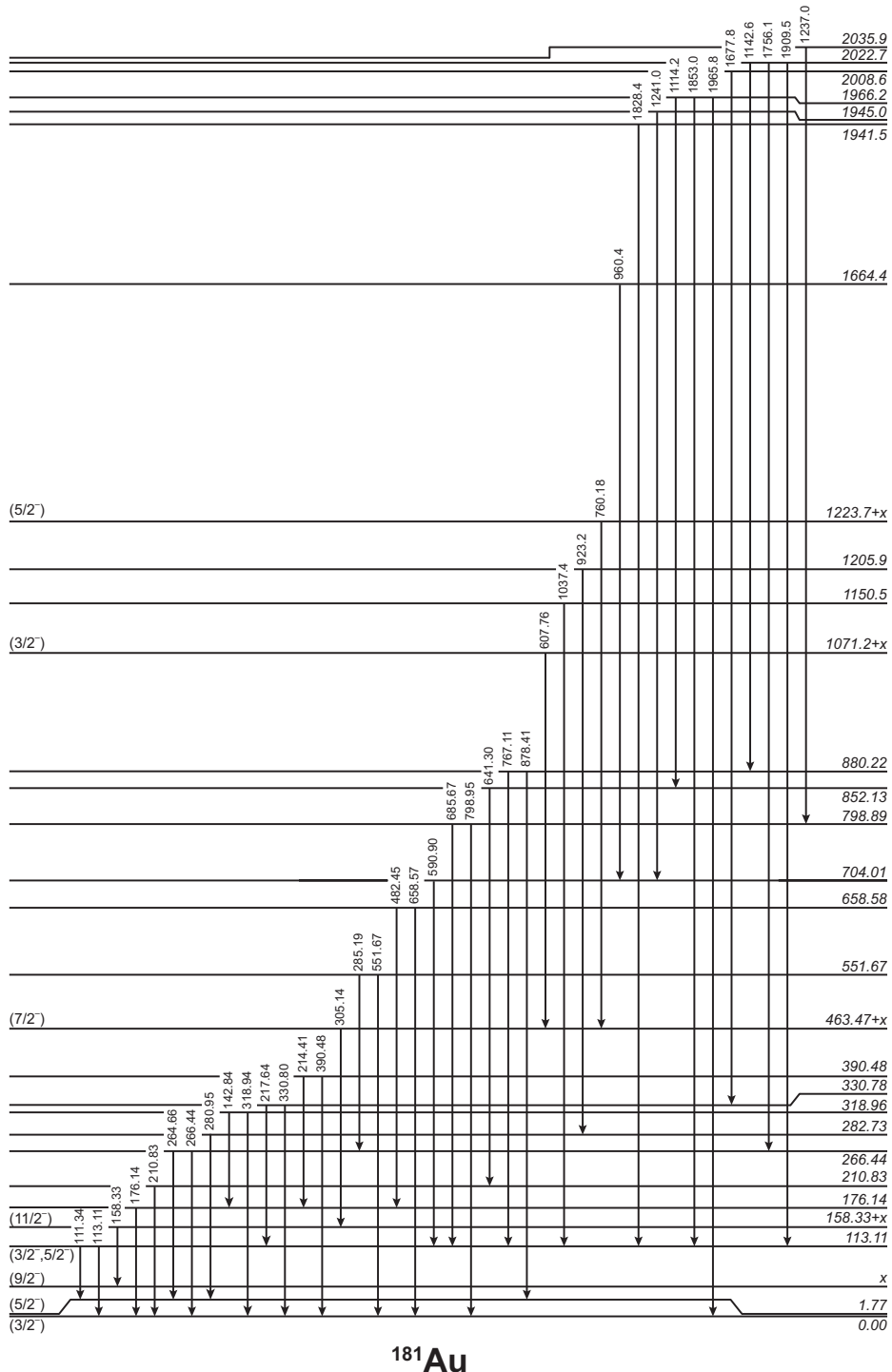


Fig. 6 Proposed level scheme of ^{181}Au as a result of the ^{181}Hg decay.

decay of the $7/2^{-}$ state feeding to $11/2^{-}$ band head. The 607.76 and 760.18 keV γ rays are interpreted as decays of the $3/2^{-}$ and the $5/2^{-}$ states, that are strongly fed in β -decay, leading to the $7/2^{-}$ state. Note that the spin-parity of the β -decaying parent ^{181}Hg is $1/2^{-}$ and therefore this sequence of γ rays must be an “inverted” spin sequence in order to feed the $11/2^{-}$ isomer.

Fig. 10 gives the projection of the $\gamma\gamma$ matrix with gate on 1142.6 keV transition. This spectrum shows 767.11 and 878.41 keV γ rays. The 767.11 keV transition is in coincidence with the 111.34 keV transition, see Fig. 8 b). The sum of 111.34 and 767.11 keV transitions, 878.45 keV, is in agreement with the 878.41 keV transition within statistical uncertainties, which give us exact location

Table 1 List of γ rays associated with decay of ^{181}Au . Uncertainties in energies are given in parentheses following the measured energy values. Uncertainties in intensities are estimated to be $\pm 20\%$ for γ rays with intensity greater or equal to 100 (set arbitrarily at the 330.80 keV line), $\pm 30\%$ for γ -ray intensities greater than or equal to 20, and $\pm 50\%$ for weaker γ rays. Transitions that were assigned to the level scheme in the present work are denoted with an asterisk. Transitions reported also in the previous study of the ^{181}Hg decay [27] are denoted with a dagger symbol. Transitions that are attributed to the α decay of ^{181}Hg are denoted with the α symbol.

E_γ [keV]	I_γ	E_γ [keV]	I_γ	E_γ [keV]	I_γ	E_γ [keV]	I_γ
111.34(4)*	205	330.80(5) ^{†,*}	100	780.01(11)	26	1246.8(1)	72
113.11(4)*	428	360.62(6)	21	782.90(20)	26	1294.2(4)	19
139.68(6)	9	388.85(10)	31	798.95(8)*	30	1331.5(1)	62
142.84(6)*	16	390.47(6)*	33	813.07(15)	11	1335.8(2)	53
147.48(4) ^{α,†}	3138	462.38(6)	28	815.13(8)	38	1409.9(1)	50
158.33(5)*	79	482.45(8)*	14	823.09(14)	16	1416.1(3)	12
165.67(4) [†]	191	519.77(6)	26	863.20(11)	15	1590.9(3)	18
176.14(4)*	354	549.79(6)	39	878.41(13)*	28	1599.3(3)	24
182.80(6)	130	551.67(5)*	79	923.2(2)*	24	1664.9(2)	46
185.77(15)	22	563.95(9)	14	930.1(2)	37	1677.8(1)*	50
191.63(5)	36	572.43(10)	11	934.6(1)	39	1691.3(3)	47
195.06(18)	16	590.90(6)*	96	960.4(1)*	153	1756.1(1)*	16
197.42(9)	34	607.76(7)*	32	973.1(2)	17	1769.1(1)	67
204.49(6)	11	629.48(6)	55	976.6(1)	50	1828.4(1)*	70
210.83(5) ^{†,*}	100	632.07(8)	28	1037.4(5)*	38	1845.0(1)	33
214.06(7) ^{α,†}	82	641.30(8)*	31	1042.1(1)	33	1853.0(1)*	41
214.41(15)*	18	658.57(9)*	27	1074.6(2)	11	1857.2(1)	26
217.64(5) ^{†,*}	30	668.77(6)	54	1111.8(2)	9	1881.6(1)	59
239.69(7) ^α	16	676.88(8)	21	1114.2(1)	22	1905.8(2)	36
264.66(5)*	67	685.67(10)*	38	1139.0(1)	43	1909.5(1)*	182
266.44(5)*	41	689.69(32)	14	1142.6(1)*	87	1957.3(1)	99
277.69(8)	13	697.88(17)	8	1150.9(2)	43	1965.8(1)*	233
280.95(5) ^{†,*}	69	702.07(23)	8	1155.0(2)	16	1979.4(1)	52
285.19(10)*	25	705.04(13)	11	1164.1(1)	20	1992.4(5)	29
305.14(5)*	35	740.88(10)	16	1169.0(1)	51	2008.0(3)	25
315.89(8)	12	743.30(20)	4	1220.6(2)	54	2019.2(1)	140
318.94(6)*	22	760.18(12)*	12	1237.0(1)*	39	2028.8(1)	149
328.93(6)	25	767.11(7)*	44	1241.0(1)*	33	2047.6(2)	14

of these transitions in the level scheme supported by coincidences.

4 Discussion

The α decay of the $^{181,183,185}\text{Au}$ isotopes was studied at the UNISOR facility [45]. While the $^{183,185}\text{Au}$ isotopes have a similar decay pattern with dominant $5/2^-$ ground-state-to-ground-state unhindered α decay, the unhindered α decay of ^{181}Au dominantly feeds the $3/2^-$ excited state [46]. This suggests a $3/2^-$ assignment for the ground state of ^{181}Au .

The observed pair of 111.34 and 113.11 keV transitions have analogues in the heavier isotopes $^{183,185}\text{Au}$, see Fig. 11. The level with spin-parity assigned as $3/2^-$ or $5/2^-$ is strongly fed with β^+/EC decay from the $1/2^-$ isomers in the Hg isobars [13,24]. This systematic pattern corroborates not only the placement of the 113.10 keV state into the level scheme with the 113.11 and 111.34 keV transition pair, but also the ground-state assignment: In $^{183,185}\text{Au}$ the stronger deexcitation

of the $(3/2^-, 5/2^-)$ state feeds the $3/2^-$ excited state, while the weaker one the $5/2^-$ ground state. In ^{181}Au , the deexcitation pattern is swapped, see Fig. 11.

Fig. 12 gives the systematics of $7/2^-$, $3/2^-$, and $5/2^-$ states of the $1h_{11/2}$ proton-hole configuration in the $^{181,183,185,187}\text{Au}$ isotopes, relative to the $11/2^-$ band head. The $9/2^-$ intruder state is also given. Excited states associated with the $1h_{11/2}$ proton-hole configuration were widely investigated in the ^{187}Au isotope [23]. Identification of 17 excited states with spins between $3/2$ and $19/2$ was reported. This includes also intruder configurations, due to coupling of the $1h_{11/2}$ proton with the excited 0^+ state in ^{188}Hg . Extensive calculations have been performed for ^{187}Au with the particle-plus-triaxial-rotor model (PTRM) [47] using a Woods-Saxon potential for the deformed mean field. These calculations suggested $\beta_2 = 0.15$ and $\gamma = 32^\circ$ deformation parameters for the ^{188}Hg core. The nearly stable trend of excited states associated with the $1h_{11/2}$ proton-hole configuration, see Fig. 12, suggests that very little is changing in lighter even-even Hg isotopes.

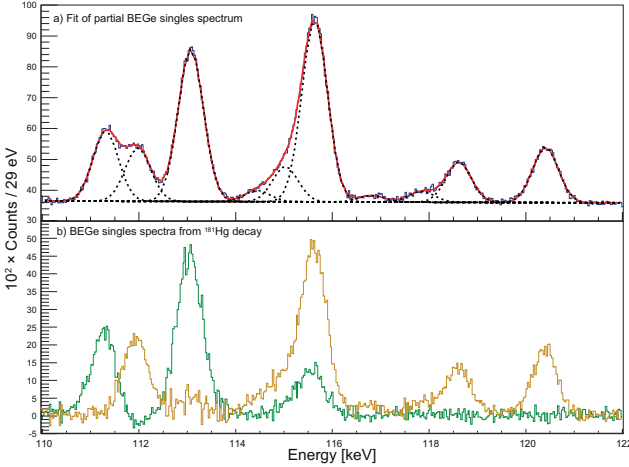


Fig. 7 a) Part of the γ -ray singles spectrum detected with the BEGe detector (blue line), a fit (red line) with multiple Gaussian peaks (black dashed line) and with linear background. b) Part of the deconvoluted singles spectra measured with the BE2020 BEGe detector. The spectrum assigned to ^{181}Hg decay is depicted by a green colour while the spectrum assigned to daughter decays is depicted by an orange line. Note that 111.34 and 113.11 keV γ rays were obscured in the previous study [28] by a much larger contamination of the 112.2 keV γ ray, which is due to the decay of the daughter isotope ^{181}Pt .

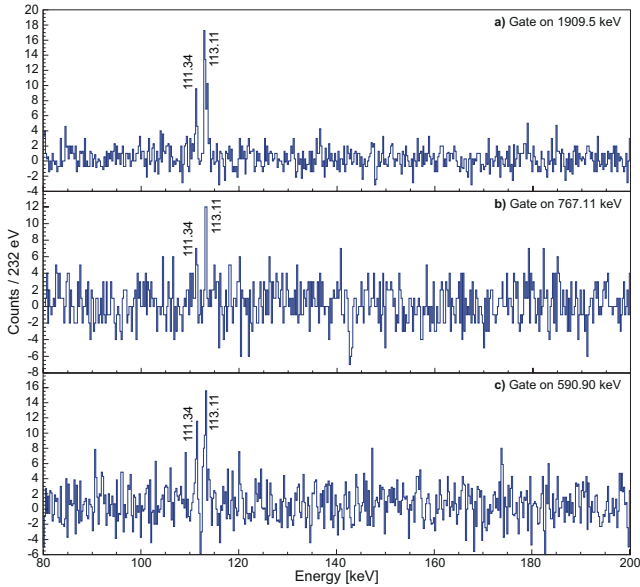


Fig. 8 Spectra of γ rays detected in a prompt coincidence with a) 1909.5 keV, b) 767.11 keV and c) 590.90 keV γ rays.

However, the PRTM model suggests that excitation energies of low-spin states, particularly $7/2^-$, $3/2^-$, and $5/2^-$ are very sensitive to changes of the triaxial deformation parameter [48]. Therefore, the slightly increasing excitation energies of these states with decreasing neutron number could indicate a slow transition from “oblatish” to “prolatish” shape in light Hg isotopes.

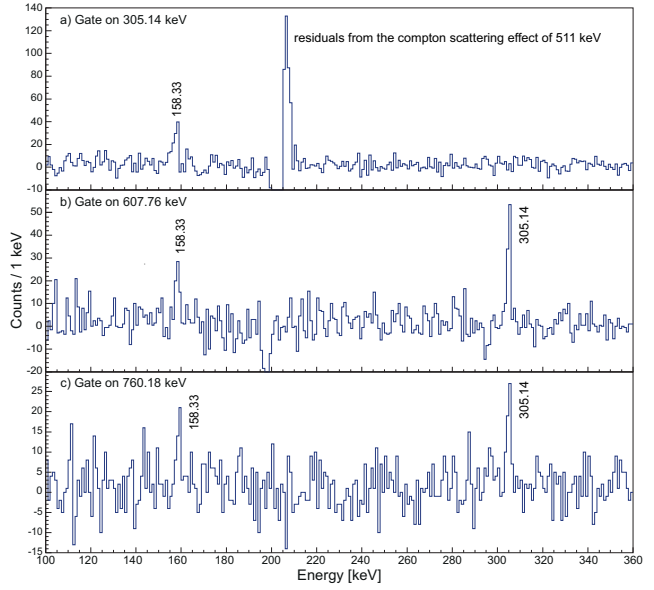


Fig. 9 Spectra of γ rays detected in a prompt coincidence with a) 305.14 keV γ rays, b) 607.76 keV γ rays and c) 760.18 keV γ rays.

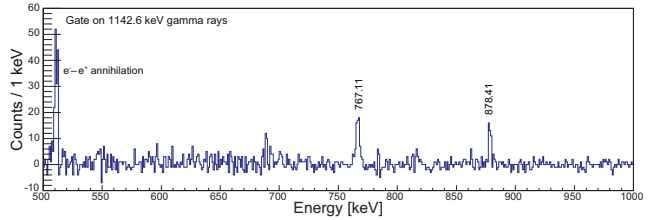


Fig. 10 Spectrum of γ rays detected in a prompt coincidence with the 1142.6 keV.

A number of strong γ rays (and many weaker γ rays) are unassigned in the decay scheme, Fig. 6. Some of these are close in energy to expected transitions between low-lying positive-parity states. Assignment of these γ rays will require higher statistics data sets. We particularly note that the lowest-energy positive-parity state will decay by an $E1$ transition and characterisation of this transition will require conversion electron spectroscopy reaching to very low energy.

5 Summary

In summary, we establish for the first time a decay scheme for $^{181}\text{Hg} \rightarrow ^{181}\text{Au}$. The main decay strength is very similar to that observed in the decays of $^{183,185}\text{Hg}$, where the β -decaying state is the same. A number of negative parity states are characterised and are shown to be consistent with a smooth systematic trend observed in heavier Au isotopes. At present, we are unable to establish any positive-parity states, although we observe unassigned γ rays with energies expected for

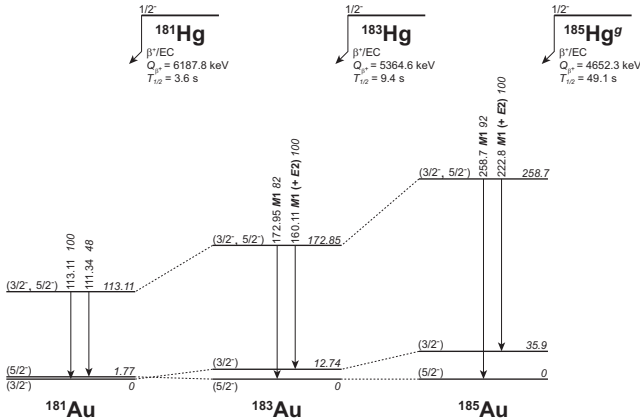


Fig. 11 Deexcitation of the $(3/2^-, 5/2^-)$ states of the $1h_{9/2} \oplus 2f_{7/2}$ configuration in the $^{181, 183, 185}\text{Au}$ isotopes. The states are strongly fed by β^+/EC decay from the corresponding low-spin isomers of the Hg isotopes, see the text for details. The data are taken from the present work and from [13, 24].

transitions between these states, based on systematic trends.

Acknowledgements The authors express their gratitude to the ISOLDE collaboration, the ISOLDE machine operators, and the CERN radioprotection team for excellent support. Special thanks go to the ISOLDE physics coordinators Magdalena Kowalska and Karl Johnston for their help. This work was supported by the Ministry of Education, Science, Research and Sport of the Slovak Republic, the Slovak Research and Development Agency under contract No. APVV-15-0225, by Slovak grant agency VEGA (contract nr. 2/0129/17), by the United Kingdom Science and Technology Facilities Council (STFC) by the EU Seventh Framework through ENSAR No. 506065, by the IUAP–Belgian Science Policy (BRix network P7/12), by GOA 10/010 from KU Leuven, and by FWO Flanders. T. E. Cocolios was supported by STFC Ernest Rutherford Fellowship No. ST/J004189/1.

References

1. J. K. Johansson, D. G. Popescu, D. D. Rajnauth, J. C. Waddington, M. P. Carpenter, L. H. Courtney, V. P. Janzen, A. J. Larabee, Z. M. Liu, L. L. Riedinger, Phys. Rev. C **40**, 132 (1989)
2. A. J. Larabee, M. P. Carpenter, L. L. Riedinger, L. H. Courtney, J. C. Waddington, V. P. Janzen, W. Nazarewicz, J.-Y. Zhang, R. Bengtsson, G. A. Léander, Physics Letters B **169**, 21 (1986)
3. P. Joshi, A. Kumar, I. M. Govil, R. P. Singh, G. Mukherjee, S. Muralithar, R. K. Bhowmik, U. Garg, Phys. Rev. C **69**, 044304 (2004)
4. W. F. Mueller, H. Q. Jin, J. M. Lewis, W. Reviol, and L. L. Riedinger, M. P. Carpenter, C. Baktash, J. D. Garrett, N. R. Johnson, I. Y. Lee, F. K. McGowan, and C.-H. Yu, S. Cwiok, Physical Review C **59**, 2009 (1999)
5. F. Soramel, P. Bednarczyk, M. Sferrazza, D. Bazzacco, D. De Acuña, G. de Angelis, M. De Poli, E. Farnea, N.H. Medina, R. Menegazzo, L. Müller, D.R. Napoli, C.M. Petrache, C. Rossi Alvarez, F. Scarlassara, G.F. Segato, C. Signorini, J. Styczeń, G. Vedovato, European Physics Journal A **4**, 17 (1999)
6. L. T. Song, X. H. Zhou, Y. H. Zhang, G. de Angelis, N. Marginean, A. Gadea, D. R. Napoli, M. Axiotis, C. Rusu, T. Martinez, Y. X. Guo, X. G. Lei, Y. Zheng, and M. L. Liu, Physical Review C **71**, 017302 (2005)
7. W. F. Mueller, W. Reviol, M. P. Carpenter, R. V. F. Janssens, F. G. Kondev, K. Abu Saleem, I. Ahmad, H. Amro, C. R. Bingham, J. Caggiano, C. N. Davids, D. Hartley, A. Heinz, B. Herskind, D. Jenkins, T. L. Khoo, T. Lauritsen, W. C. Ma, J. Ressler, L. L. Riedinger, D. G. Sarantites, D. Seweryniak, S. Siem, A. A. Sonzogni, J. Uusitalo, P. G. Varmette, I. Wiedenhöver, and R. Wadsworth, Physical Review C **69**, 064315 (2004)
8. L. T. Song, X. H. Zhou, Y. H. Zhang, Y. X. Guo, X. G. Lei, Z. Y. Sun, M. Oshima, T. Toh, A. Osa, M. Koizumi, J. Kataura, Y. Hatsukawa, M. Matsuda, and M. Sugawara, Physical Review C **69**, 037302 (2004)
9. P. Joshi, A. Kumar, G. Mukherjee, R. P. Singh, S. Muralithar, U. Garg, R. K. Bhowmik, I. M. Govil, Phys. Rev. C **66**, 044306 (2002)
10. F. G. Kondev, P. Carpenter, V. F. Janssens, K. Abu Saleem, I. Ahmad, H. Amro, J. A. Cizewski, M. Danchev, C. N. Davids, D. J. Hartley, A. Heinz, T. L. Khoo, T. Lauritsen, C. J. Lister, W. C. Ma, G. L. Poli, J. J. Ressler, W. Reviol, L. L. Riedinger, D. Seweryniak, M. B. Smith, I. Wiedenhöver, Physics Letters B **512**(3), 268 (2001)
11. F. G. Kondev, M. P. Carpenter, R. V. F. Janssens, K. Abu Saleem, I. Ahmad, M. Alcorta, H. Amro, J. Caggiano, J. A. Cizewski, M. Danchev, C. N. Davids, D. J. Hartley, A. Heinz, B. Herskind, R. A. Kaye, T. L. Khoo, T. Lauritsen, C. J. Lister, W. C. Ma, G. L. Poli, J. J. Ressler, W. Reviol, L. L. Riedinger, D. Seweryniak, S. Siem, M. B. Smith, A. A. Sonzogni, P. G. Varmette, I. Wiedenhöver, Nuclear Physics A **682**, 487 (2001)
12. M. P. Carpenter, F. G. Kondev, R. V. F. Janssens, D. Jenkins, K. Abu Saleem, I. Ahmad, H. Amro, A. N. Andreyev, J. Caggiano, J. A. Cizewski, M. Danchev, C. N. Davids, T. Enqvist, P. T. Greenlees, A. Heinz, P. Herskind, P. M. Jones, D. T. Joss, R. Julin, S. Juutinen, H. Kettunen, T. L. Khoo, P. Kuusiniemi, P., AIP Conference Proceedings **656**, 55 (2003)
13. M. Venhart, F. A. Ali, W. Ryssens, J. L. Wood, D. T. Joss, A. N. Andreyev, K. Auranen, B. Bally, M. Balogh, M. Bender, R. J. Carroll, J. L. Easton, P. T. Greenlees, T. Grahn, P.-H. Heenen, A. Herzán, U. Jakobsson, R. Julin, S. Juutinen, D. Klč, J. Konki, E. Lawrie, M. Leino, V. Matoušek, C. G. McPeake, D. O'Donnell, R. D. Page, J. Pakarinen, J. Partanen, P. Peura, P. Rahkila, P. Ruotsalainen, M. Sandzelius, J. Sarén, B. Saygi, M. Sedláček, C. Scholey, J. Sorri, S. Stolze, A. Thorntwaite, J. Uusitalo, and M. Veselský, Physical Review C **95**, 061302 (2017)
14. H. Watkins, D. T. Joss, T. Grahn, R. D. Page, R. J. Carroll, A. Dewald, P. T. Greenlees, M. Hackstein, R.-D. Herzberg, U. Jakobsson, P. M. Jones, R. Julin, S. Juutinen, S. Ketelhut, T. Kröll, R. Krücke, M. Labiche, M. Leino, N. Lumley, P. Maierbeck, M. Nyman, P. Nieminen, D. O'Donnell, J. Ollier, J. Pakarinen, P. Peura, T. Pissulla, P. Rahkila, J. P. Revill, W. Rother, P. Ruotsalainen, S. V. Rigby, J. Sarén, P. J. Sapple, M. Scheck, C. Scholey, J. Simpson, J. Sorri, J. Uusitalo, and M. Venhart, Physical Review C **84**, 051302 (2011)
15. T. Grahn, H. Watkins, D. T. Joss, R. D. Page, R. J. Carroll, A. Dewald, P. T. Greenlees, M. Hackstein, R.-D. Herzberg, U. Jakobsson, P. M. Jones, R. Julin, S. Juutinen, S. Ketelhut, T. Köll, R. Krücke, M. Labiche, M.

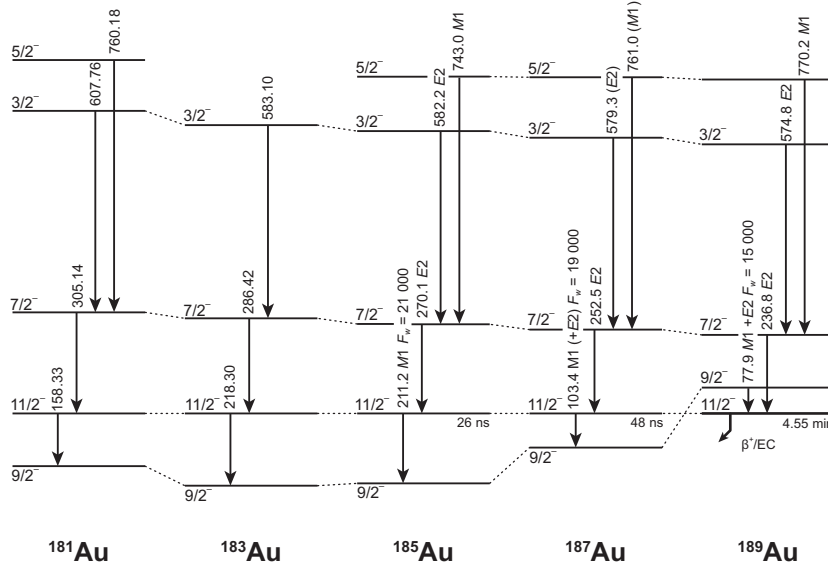


Fig. 12 Systematics of the $7/2^-$, $3/2^-$, and $5/2^-$ states associated with the $1h_{11/2}$ proton-hole configuration.

- Leino, N. Lumley, P. Maierbeck, M. Nyman, P. Nieminen, D. O'Donnell, J. Ollier, J. Pakarinen, P. Peura, T. Pissulla, P. Rahkila, J. P. Revill, W. Rother, P. Ruotsalainen, S. V. Rigby, J. Sarén, P. J. Sapple, M. Scheck, C. Scholey, J. Simpson, J. Sorri, J. Uusitalo, M. Venhart, Journal of Physics: Conference Series **420**, 012047 (2013)
16. T. Bäck, B. Cederwall, K. Lagergren, R. Wyss, R. A. Johnson, D. Karlsgren, P. T. Greenlees, D. G. Jenkins, P. Jones, D.T. Joss, R. Julin, S. Juutinen, A. Keenan, H. Kettunen, P. Kuusiniemi, M. Leino, A.-P. Leppänen, M. Muikku, P. Nieminen, J. Pakarinen, P. Rahkila, J. Uusitalo, The European Physical Journal A - Hadrons and Nuclei **16**, 489 (2003)
 17. M. B. Smith, J. A. Cizewski, M. P. Carpenter, F. G. Kondev, R. V. F. Janssens, K. Abu Saleem, I. Ahmad, H. Amro, M. Danchev, C. N. Davids, D. J. Hartley, A. Heinz, T. L. Khoo, T. Lauritsen, C. J. Lister, W. C. Ma, G. L. Poli, J. J. Ressler, W. Reviol, L. L. Riedinger, D. Seweryniak, I. Wiedenhöver, Nuclear Physics A **682**, 433 (2001)
 18. E. Gueorguieva, C. Schück, A. Minkova, Ch. Vieu, F. Hannachi, M. Kaci, M.-G. Porquet, R. Wyss, J. S. Dionisi, A. Korichi, and A. Lopez-Martens, Phys. Rev. C **68**, 054308 (2003)
 19. E. F. Zganjar, J. L. Wood, R. W. Fink, L. L. Riedinger, C. R. Bingham, B. D. Kern, J. L. Weil, J. H. Hamilton, A. V. Ramayya, E. H. Spejewski, R. L. Mlekodaj, H. K. Carter, W. D. Schmidt-Ott, Physics Letters B **58**, 159 (1975)
 20. J. L. Wood, R. W. Fink, E. F. Zganjar, J. Meyer-ter-Vehn, Physical Review C **14**, 682 (1976)
 21. J. L. Wood, M. O. Kortelahti, E. F. Zganjar, P. B. Semmes, Nuclear Physics A **600**, 283 (1996)
 22. D. Rupnik, E. F. Zganjar, J. L. Wood, P. B. Semmes, W. Nazarewicz, Phys. Rev. C **51**, R2867 (1995)
 23. D. Rupnik, E. F. Zganjar, J. L. Wood, P. B. Semmes, P. F. Mantica, Physical Review C **58**, 771 (1998)
 24. M. O. Kortelahti, E. F. Zganjar, H. K. Carter, C. D. Papanicopoulos, M. A. Grimm, J. L. Wood, Journal of Physics G: Nuclear Physics **14**, 1361 (1988)
 25. C. D. Papanicopoulos, M. A. Grimm, J. L. Wood, E. F. Zganjar, M. O. Kortelahti, J. D. Cole, H. K. Carter, Zeitschrift für Physik A Atomic Nuclei **330**(4), 371 (1988)
 26. M. Venhart, J. L. Wood, M. Sedlák, M. Balogh, M. Bírová, A. J. Boston, T. E. Cocolios, L. J. Harkness-Brennan, R.-D. Herzberg, L. Holub, D. T. Joss, D. S. Judson, J. Klíman, J. Klímo, L. Krupa, J. Lušnák, L. Makhathini, V. Matoušek, Š. Motyčák, R. D. Page, A. Patrل, K. Petrík, A. V. Podshibyakin, P. M. Prajapati, A. M. Rodin, A. Špaček, R. Urban, C. Unsworth, M. Veselský, Journal of Physics G: Nuclear and Particle Physics **44**, 074003 (2017)
 27. J. Sauvage, C. Bourgeois, P. Kilcher, F. Le Blanc, B. Roussi  re, M. I. Macias-Marques, F. Bragan  a Gil, H. G. Porquet, H. Dautet, Nuclear Physics A **540**, 83 (1992)
 28. M. I. Macias-Marques, C. Bourgeois, P. Kilcher, B. Roussi  re, J. Sauvage, M. C. Abreu, M. G. Porquet, Nuclear Physics A **427**, 205 (1984)
 29. C. Bourgeois and P. Kilcher and B. Roussi  re and J. Sauvage-Letessier and M.G. Porquet, Nuclear Physics A **386**, 308 (1982)
 30. C. Ekstr  m, I. Lindgren, S. Ingelman, M. Olmats, G. Wannberg, Physics Letters B **60**, 146 (1976)
 31. C. Ekstr  m and L. Robertsson and S. Ingelman and G. Wannberg and I. Ragnarsson, Nuclear Physics A **348**, 25 (1980)
 32. K. Wallmeroth, G. Bollen, A. Dohn, P. Egelhof, U. Kr  nert, M.J.G. Borge, J. Campos, A.Rodriguez Yunta, K. Heyde, C. De Coster, J. L. Wood, H.-J. Kluge, Nuclear Physics A **493**, 224 (1989)
 33. J. G. Cubiss, A. E. Barzakh, A. N. Andreyev, M. Al Monteny, N. Althubiti, B. Andel, S. Antalic, D. Atanasov, K. Blaum, T.E. Cocolios, T. Day Goodacre, R. P. de Groot, A. de Roubin, G. J. Farooq-Smith, D. V. Fedorov, V. N. Fedossev, R. Ferrer, D. A. Fink, L. P. Gaffney, L. Ghys, A. Gredley, R. D. Harding, F. Herfurth, M. Huyse, N. Imai, D.T. Joss, U. K  ster, S. Kreim, V. Liberati, D. Lunney, K. M. Lynch, V. Manea, B. A. Marsh, Y. Martinez Palenzuela, P. L. Molkanov, P. Mosat, D. Neidherr, G. G. O'Neill, R. D. Page, T. J. Procter, E. Rapisarda, M. Rosenbusch, S. Rothe, K. Sandhu, L. Schweikhard, M.D. Seliverstov, S. Sels, P. Spagnoli, V. L. Truesdale, C. Van Beveren, P. Van Duppen, M. Veinhard, M. Venhart, M. Veselsk  , F. Wearing, A. Welker, F. Wienholtz, R. N. Wolf, S. G. Zemlyanoy, K. Zuber, Physics Letters B **786**, 355 (2018)

34. A. N. Andreyev, S. Antalic, D. Ackermann, T. E. Cocolios, V. F. Comas, J. Elseviers, S. Franchoo, S. Heinz, J. A. Heredia, F. P. Hessberger, S. Hofmann, M. Huyse, J. Khuyagbaatar, I. Kojouharov, B. Kindler, B. Lommel, R. Mann, R. D. Page, S. Rinta-Antila, P. J. Sapple, Š. Šáro, P. Van Duppen, M. Venhart, and H. V. Watkins, Phys. Rev. C **80**, 024302 (2009)
35. M. Venhart, A. N. Andreyev, J.L. Wood, S. Antalic, L. Bianco, P.T. Greenlees, U. Jakobsson, P. Jones, R. Julin, S. Juutinen, S. Ketelhut, M. Leino, M. Nyman, R. D. Page, P. Peura, P. Rahkila, J. Sarén, C. Scholey, J. Sorri, J. Thomson, J. Uusitalo, Physics Letters B **695**, 82 (2011)
36. G. D. Dracoulis, G. J. Lane, H. Watanabe, R. O. Hughes, N. Palalani, F. G. Kondev, M. P. Carpenter, R. V. F. Janssens, T. and Lauritsen, C. J. Lister, D. Seweryniak, S. Zhu, P. Chowdhury, W. Y. Liang, Y. Shi, F. R. Xu, Physical Review C **87**, 014326 (2013)
37. K. Heyde and P. Van Isacker and M. Waroquier and J.L. Wood and R.A. Meyer, Physics Reports **102**, 291 (1983)
38. J. L. Wood and K. Heyde and W. Nazarewicz and M. Huyse and P. van Duppen, Physics Reports **215**, 101 (1992)
39. Heyde, Kris and Wood, John L., Rev. Mod. Phys. **83**, 1467 (2011)
40. M. Venhart, J. L. Wood, A.J. Boston, T.E. Cocolios, L.J. Harkness-Brennan, R.-D. Herzberg, D.T. Joss, D.S. Judson, J. Kliman, V. Matoušek, Š. Motyčák, R. D. Page, A. Patel, K. Petřík, M. Sedlák, M. Veselský, Nuclear Instruments and Methods in Physics Research Section A: Accelerators, Spectrometers, Detectors and Associated Equipment **849**, 112 (2017)
41. V. Matoušek, M. Sedlák, M. Venhart, D. Janičovič, J. Kliman, K. Petřík, P. Švec, P. Švec, M. Veselský, Nuclear Instruments and Methods in Physics Research Section A: Accelerators, Spectrometers, Detectors and Associated Equipment **812**, 118 (2016)
42. L. J. Harkness-Brennan, D.S. Judson, A. J. Boston, H. C. Boston, S. J. Colosimo, J. R. Cresswell, P. J. Nolan, A. S. Adekola, J. Colaresi, J. F. C. Cocks, W. F. Mueller, Nuclear Instruments and Methods in Physics Research Section A: Accelerators, Spectrometers, Detectors and Associated Equipment **760**, 28 (2014)
43. E. Hagberg and P.G. Hansen and P. Hornshøj and B. Jonsson and S. Mattsson and P. Tidemand-Petersson, Nuclear Physics A **318**, 29 (1979)
44. B. L. Ader and N. N. Perrin, Nuclear Physics A **307**, 189 (1972)
45. C. R. Bingham, M. B. Kassim, M. Zhang, Y. A. Akovali, K. S. Toth W. D. Hamilton, H. K. Carter, J. Kormicki, J. von Schwarzenberg, M. M. Jarrio, Physical Review C **51**, 125 (1995)
46. F. Meissner, H. Salewski, W.-D. Schmidt-Ott, U. Bosch-Wicke, V. Kunze, R. Michaelsen, Physical Review C **48**, 2089 (1993)
47. S. E. Larsson and G. A. Leander and I. Ragnarsson, Nucl. Phys. A **307**, 189 (1978)
48. J. Meyer-ter-Vehn and F. S. Stephens and R. M. Diamond, Phys. Rev. Lett. **32**, 1383 (1974)